Powder Metallurgy and Metal Ceramics, Vol. 55, Nos. 5-6, September, 2016 (Russian Original Vol. 55, Nos. 5-6, May-June, 2016)

STRUCTURAL PHASE TRANSFORMATIONS IN $Zr_{50}Co_{25}Ni_{25}$ ALLOY

O. L. Semenova,[1,3] J.-C. Tedenac,[2] and O. S. Fomichev[1]

UDC 669.017.3

High-temperature X-ray diffraction is applied to study for the first time the structural phase transformations in the $Zr_{50}Co_{25}Ni_{25}$ alloy at 30–800°C. It is shown that this alloy contains one phase at room temperature, with an orthorhombic crystal structure of CrB type. When temperature increases to 400°C, this phase transforms into a tetragonal phase of AuCu type. A phase with a cubic crystal structure of CsCl type and a monoclinic one of TiNi type show up at 800°C. The TiNi-type phase remains up to room temperature when the sample is cooled down.

Keywords: *crystal structure, phase, high-temperature martensitic transformations.*

INTRODUCTION

The mechanical properties of ZrCo–ZrNi alloys attract special research attention. This is reasoned by the apparent but somewhat limited ductility of the equiatomic ZrCo binary alloy, which greatly improves in ternary alloys where cobalt is replaced by nickel [1–9].

Along with the above, solid-state transformations that proceed in the alloys in the temperature range –183…–867°C were studied in [1–5]. The data were obtained using the temperature dependence of electrical resistivity, magnetic susceptibility, and dilatometry as physicochemical analysis methods. The paper [5] was the first to determine the structure of alloys in this section at room temperature. It is shown that in spite of close atomic radii of Co and Ni (0.2504 and 0.2492 nm), the mutual solubility between the equiatomic compounds formed by these metals and zirconium is limited, and two solid solutions are observed at room temperature: based on ZrCo with a cubic structure of CsCl type (to 14 at.% Ni) and based on ZrNi with an orthorhombic structure of CrB type (16–50 at.% Ni). The alloys containing 10–30 at.% Ni undergo a solid-state transformation, which is of martensitic nature according to metallographic analysis [1]. The papers [6–9] examine the relation between the microstructure and mechanical properties of the alloys. It is concluded that ductility of the alloy improves extraordinarily when cobalt is replaced by 11 at.% Ni because the matrix cubic phase undergoes transformation.

These data were used in [10, 11] to verify whether the Zr_2CoNi structure at room temperature belonged to B19 or B19′ type peculiar to compounds resulting from transformation of CsCl-type phases. The existence of two martensitic phases, belonging to space groups $P2_1/m$ (19′ type) and *Cmcm*, in the Zr_2CoNi alloy at room temperature was assumed in [10, 11]. Then this assumption was confirmed in [12] for the alloy close to Zr_2CoNi

[1]Frantsevich Institute for Problems of Materials Science, National Academy of Sciences of Ukraine, Kiev, Ukraine. [2]University of Montpellier, Montpellier, France.

[3]To whom correspondence should be addressed; e-mail: selena@ipms.kiev.ua.

Translated from Poroshkovaya Metallurgiya, Vol. 55, Nos. 5–6 (509), pp. 111–119, 2016. Original article submitted December 25, 2014.

stoichiometry, and lattice parameters of these phases were calculated. It is also shown that the martensitic transformation in the Zr_2CoNi alloy is accompanied by the shape memory effect with critical transformation temperatures M_s = 620°C, M_s = 480°C, A_s = 700°C, and A_f = 950°C [10, 11].

Data on the martensitic transformation in the Zr_2CoNi alloy at 620–950°C [10, 11] and data [6–9] on the relation between the ductility and microstructure of the alloys testify that variation in crystal structure is dependent not only on alloy composition [1–9] but also temperature.

For deeper understanding of the phase transformations and their relation to macroscopic behavior (mechanical properties), we observed changes in the crystal structure of the ZrCo–ZrNi alloys (in particular, $Zr_{50}Co_{25}Ni_{25}$) when the sample was heated and cooled down from room temperature to 800°C.

EXPERIMENTAL PROCEDURE

The starting materials for the $Zr_{50}Co_{25}Ni_{25}$ alloy were iodide-refined zirconium and electrolytic cobalt and nickel of 99.95% purity. The alloy was melted in an arc furnace on a water-cooled copper hearth in a purified argon atmosphere directly from the components. The melting losses were no more than 0.5% and the alloy composition was accepted in accordance with the starting charge. Changes in the alloy crystal structure were studied by high-temperature X-ray diffraction in a range from room temperature to 1000°C when the sample was heated and cooled down. The X-ray diffraction patterns were taken from a thin section of a massive sample employing a Seifert/Philips PW 1050 diffractometer in Cu-K_α radiation in a high-temperature Ahton Paar HTK 16 chamber. The X-ray diffraction patterns obtained at 30, 200, 400, 600, and 800°C were processed with the Powder Cell 2.4 software. The thermal curves were plotted using a differential thermal analysis unit, designed and fabricated by the Department for Physical Chemistry of Inorganic Materials at the Frantsevich Institute for Problems of Materials Science, with a W–W/Re wire thermocouple at a rate of 20°/min in the temperature range 300–1300°C [13]. To identify the effect corresponding to the solid-state transformation, a blind hole was drilled in the sample into which the thermocouple was placed so that it directly touched the sample. The measurement error was 1%.

EXPERIMENTAL RESULTS AND DISCUSSION

The chemical composition of the $Zr_{50}Co_{25}Ni_{25}$ alloy determined by scanning a thin section over an area of 1.1 mm^2—50.12 at.% Zr–23.75 Co–26.13 at.% Ni—indicates that there is some deviation from 50 at.% Zr. The microstructure of the as-cast alloy (Fig. 1) thus shows precipitates surrounding the primary phase grains. The sample begins melting with this component at 1271°C, followed by melting of the matrix phase at 1286°C (Fig. 2*a*). That there is a small amount of the component whose parts crystallize between primary phase grains is confirmed, besides metallography, by thermal analysis (little difference in the solidus temperatures and phase transformation

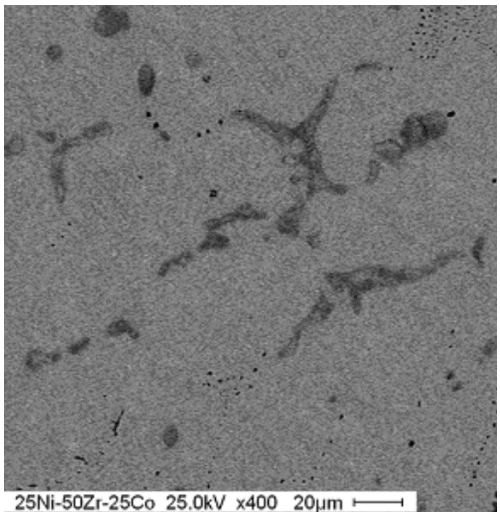

Fig. 1. Microstructure of the as-cast $Zr_{50}Co_{25}Ni_{25}$ alloy

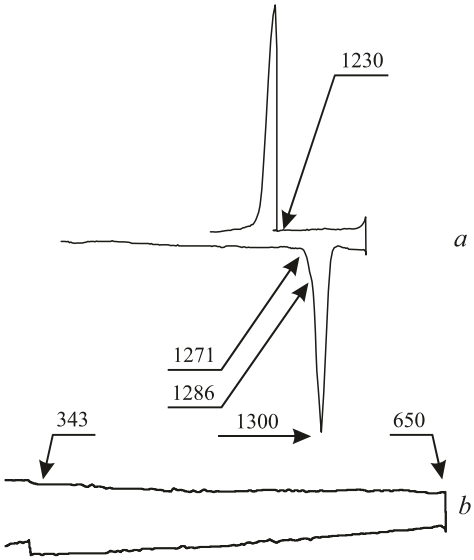

Fig. 2. Thermal curves for the $Zr_{50}Co_{25}Ni_{25}$ alloy in the range of melting–crystallization temperatures (*a*) and 300–650°C (*b*)

temperatures) and electron microprobe analysis (EMPA) data on composition of the primary phase, being 50.25 at.% Zr–25.52 Co–24.22 at.% Ni. Taking into account the experimental error (1–2 at.%), this composition does not differ much from the general composition of the sample. Data from EMPA for the intergrain constituent lead to a conclusion that it includes a binary Laves $ZrCo_2$ phase.

X-ray diffraction results for the alloys for 30–800°C are provided in Table 1. The X-ray diffraction spectra for the alloy at 30 and 200°C obtained during heating are similar and can be identified as those that describe one phase (δ″) with an orthorhombic structure of CrB type (space group *Cmcm*) (Fig. 3). Figure 4*a* shows a fragment of the X-ray diffraction pattern to demonstrate how much the theoretical and experimental intensities of the spectrum lines agree at 30°C. We see that agreement between the theoretical and experimental diffraction patterns is not very satisfactory.

TABLE 1. Phase Composition and Lattice Parameters of Phases (nm) in the $Zr_{50}Co_{25}Ni_{25}$ Alloy at 30–800°C

T, °C	Alloy phase composition	δ″			δ′	
		a	*b*	*c*	*a*	*b*
Heating						
30	δ″	0.3264 ± 2	0.9842 ± 2	0.4155 ± 2	–	–
200	δ″	0.3271 ± 2	0.9837 ± 2	0.4159 ± 2	–	–
400	δ″ + δ′	0.3290 ± 1	0.981 ± 1	0.4156 ± 6	0.510 ± 1	0.519 ± 1
600	δ″ + δ′	0.324	0.983	0.408	0.511 ± 1	0.521 ± 1
T, °C	Alloy phase composition	δ	δ‴			
		a	*a*	*b*	*c*	β, deg
Cooling						
800	δ‴ + δ	0.303	0.2912 ± 3	0.404 ± 1	0.471 ± 1	97.6
600	δ‴	–	0.2895 ± 4	0.399 ± 2	0.4725 ± 6	97.6
400	δ‴	–	0.2889 ± 4	0.402 ± 2	0.4715 ± 6	97.4
200	δ‴	–	0.2886 ± 3	0.404 ± 1	0.4710 ± 4	97.54
30	δ‴	–	0.2885 ± 3	0.404 ± 1	0.4710 ± 4	97.6

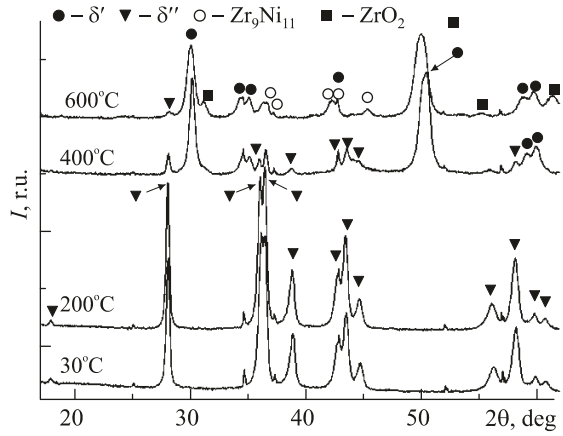

Fig. 3. X-ray diffraction patterns for the $Zr_{50}Co_{25}Ni_{25}$ alloy in heating to 30–600°C

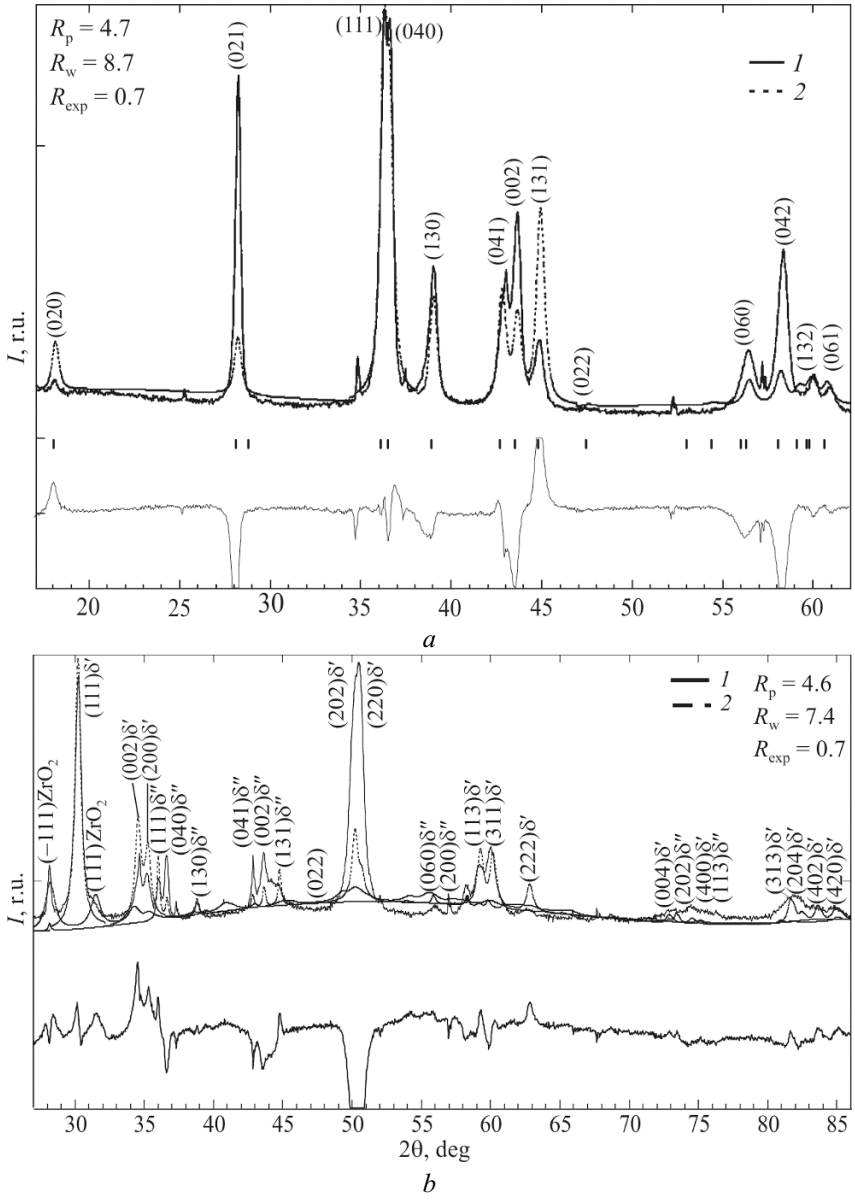

Fig. 4. Agreement between the theoretical and experimental diffraction patterns for the $Zr_{50}Co_{25}Ni_{25}$ alloy at 30°C (*a*) and 400°C (*b*): *1*) experimental, *2*) theoretical

The increased intensities of reflections (0k0) in the experimental patterns compared to those in the theoretical ones can be indicative of predominant grain orientation in direction [010], perpendicular to the thin section. After the texture in this direction was taken into account, agreement between the intensities of theoretical and experimental diffraction patterns somewhat improved, but the integral intensities of reflections (021) and (042) still did not match with the experimental ones. Several texture options were tested, including one with axis [021]. The option of the texture with axis [021] turned out to be less satisfactory, so we gave preference to the texture with axis [010] and thus reached much better R factors. The texture factor is 0.8. The lattice parameters of the CrB-type phase (δ″) weakly depend on temperature within the error of measurement (Fig. 4*a*, *b*; Table 1). This result differs from the X-ray diffraction data [13] for the alloy whose initial charge includes 25.5 at.% Ni and in which, besides the phase with an orthorhombic structure and lattice parameters close to ours, a phase with a monoclinic structure of B19′ type was identified, its amount being predominant in this alloy (~60%) according to [12]. The X-ray diffraction pattern for the $Zr_{50}Co_{25}Ni_{25}$ alloy provided in [12] has no independent line that could belong to the B19′ phase spectrum. It is likely that the spectrum of this phase was involved in [12] to improve the R factors (X-ray diffraction pattern provided in [12] shows no independent reflections of the B19′ phase in this alloy), but this cannot be adequate evidence that the B19′ phase exists in this alloy.

The X-ray diffraction patterns for the $Zr_{50}Co_{25}Ni_{25}$ alloy taken at 30 and 200°C have also several peaks of low intensity at 2θ ~ 26°, ~35, ~37, and 2θ ~ 52°, which do not belong to the orthorhombic phase spectrum and were not identified by us (Fig. 3). Their appearance may result from the capability of the Co–Ni–Zr ternary alloys, Co–Zr and Ni–Zr binary alloys, and alloys in the ZrCo–ZrNi section to transform easily to metastable state both when cooled and deformed (for example, in the production of thin sections). These low-intensity peaks in the X-ray diffraction patterns for the $Zr_{50}Co_{25}Ni_{25}$ alloy at 30 and 200°C disappear when it is further heated to 600 and 800°C.

The X-ray diffraction pattern obtained at 400°C includes spectra of two phases (Figs. 3 and 4*b*). In addition to peaks of the low-temperature phase (δ″) with smaller intensity compared to that at 30 and 200°C (which testifies that amount of this phase decreases), there are peaks at reflection angles that correspond to the tetragonal structure of AuCu type (space group *P*4/*mmm*) and characterize the δ′ phase. The tetragonal phase is the main one in the alloy at 400°C (Fig. 4*b*; Table 1). The X-ray diffraction pattern for the alloy at 400°C has peaks being indicative of one more phase. They belong to the ZrO_2 oxide phase with a monoclinic structure and lattice parameters determined with an accuracy of 0.001 nm: $a = 0.517$ nm, $b = 0.519$ nm, and $c = 0.535$ nm; $\beta = 99.0°$.

The δ′ phase peaks become more intensive when the sample is heated further to 600°C, while those of the orthorhombic phase become less intensive (Fig. 3). Besides these phases, a series of reflections show up at 600°C, which can be identified as the tetragonal Zr_9Ni_{11} phase. This phase may appear when some amount of zirconium oxidizes and composition of the equiatomic phase shifts toward composition of the closest phase with higher nickel content of Zr_9Ni_{11} stoichiometry. This is a tetragonal phase with structure *I*4/*m* [14] and lattice parameters $a = 1.09 \pm 0.001$ nm and $c = 0.702 \pm 0.01$ nm at 800°C. The appearance of these two phases testifies that composition of the alloy studied extends away from the ZrCo–ZrNi quasibinary section.

The ZrCo–ZrNi system containing the $Zr_{50}Co_{25}Ni_{25}$ alloy is a quasibinary section of the Zr–Co–Ni ternary system. Such sections have properties of binary phase diagrams; hence, the $Zr_{50}Co_{25}Ni_{25}$ equilibrium alloy should include no more than two phases at 600 and 800°C. The ZrO_2 and Zr_9Ni_{11} phases characterize the Zr–Co–Ni–O quaternary system. Further review of transformations in the alloy when cooled down will ignore the phases that do not result from martensitic transformations. The Zr_9Ni_{11} phase remains in the alloy when heated to 800°C and then cooled down.

Peaks of the oxide phase become more intensive when temperature increases to 800°C and the sample is further cooled. This indicates that long exposure at high temperatures leads to its greater oxidation (Fig. 5). The amount of the oxide phase at 800°C is ~70 wt.%, significantly complicating the identification of other phases present in the sample and increasing the error in calculating the lattice parameters.

The X-ray diffraction pattern for the $Zr_{50}Co_{25}Ni_{25}$ alloy at 800°C no longer shows lines of the δ″ phase, whose amount decreases during heating from 30 to 600°C. The only independent reflection typical of the δ′ phase,

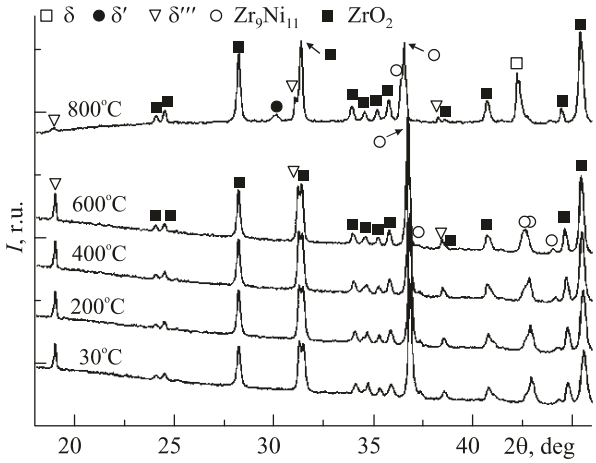

Fig. 5. X-ray diffraction pattern for the $Zr_{50}Co_{25}Ni_{25}$ alloy in cooling from 800 to 30°C

(111), cannot be reliable evidence of its existence at this temperature. Instead, there are new peaks that correspond to the diffraction spectra of monoclinic TiNi (δ‴) and cubic CsCl (δ). The latter results from transformation of the δ′ phase (Table 1, Fig. 5). This phase should be logically expected to appear in the alloy at higher temperatures because one of the components, ZrCo, has the same crystal structure and dissolves more than 25 at.% Ni at subsolidus temperature [12]. This is also testified by the phase composition and transformation temperature of the alloys with 0–16 at.% Ni determined by X-ray diffraction and thermal analysis [6]. The transformation temperature tends to increase with higher nickel content and A_f is 345°C for the alloy with 16 at.% Ni.

The coexistence of the δ and δ‴ phases at 800°C indicates that the δ matrix phase transforms to the δ‴ phase in this alloy at temperatures higher than 800°C. The likely presence of the δ′ phase at 800°C, in addition to the δ and δ‴ phases, is indicative of gradual change in the crystal lattice and extended temperature range of the process. The application of physicochemical analysis properties such as temperature dependence of magnetic susceptibility and electrical resistivity to reveal transformations in the ZrCo–ZrNi alloy [3, 4] has shown that effects on these dependences, corresponding to solid-state transformations, become less pronounced and their temperature increases with higher nickel content. The alloy with 20 at.% Ni exhibits only a bend on the temperature dependence of resistivity, becoming smooth in transition to the alloy with 30 at.% Ni. We believed that the bend on the thermal curve of the $Zr_{50}Co_{25}Ni_{25}$ alloy at 345°C, corresponding to the existence range of the δ″ + δ′ phases, was also a sign of similar transformation [15]. However, considering that there are no signs of thermomechanical transformation in this alloy and addressing the data reported in [3, 4], we have concluded that this bend is not evidence of the $\delta'' \rightarrow \delta^*$ transformation.

The X-ray diffraction patterns of the alloy when cooled down at 800°C are similar but substantially differ from those taken when the alloy is heated. The oxide phase peaks overlapped with those belonging to the δ′ phase at 600 and 400°C (Fig. 5); hence, existence of the δ′ phase in the alloy at this cooling temperature has not been determined reliably. The most likely assumption is that the final product of the martensitic $\delta \rightarrow \delta'''$ transformation forms immediately, and the monoclinic TiNi-type phase remains in the alloys at 600, 400, 200, and 30°C (Fig. 5). Therefore, the low-symmetry monoclinic TiNi-type phase is equilibrium structure at room temperature (30°C) after holding at high temperatures rather than orthorhombic CrB-type phase present in the starting alloy; i.e., annealing of the alloy gave rise to a phase with another equilibrium structure. Table 1 shows that lattice parameters of this phase do not change with temperature but differ from those determined in [12] for the alloy at room temperature without annealing. It should be added that, according to [16], variation in alloy composition (in our case, appearance of two phases, ZrO_2 and Zr_9Ni_{11}) can lead to another way of transformations and thus influence properties of the final

[*] The $Zr_{50}Co_{25}Ni_{25}$ alloy was tested by three-point bending at the Kurdyumov Institute for Metal Physics, National Academy of Sciences of Ukraine, by researcher Yu. V. Kudryavtsev.

product. However, as the two phases appear when the alloy oxidizes in the heating process, they do not apparently influence the result of martensitic transformation of the high-temperature δ phase.

The X-ray diffraction patterns for the cooling process show abnormally high intensity (compared to theoretical one) of reflections (h00) peculiar to the monoclinic structure, indicating that the sample is textured in direction [100] (Fig. 5). The texture factor is ~0.3. If we consider that the monoclinic TiNi-type structure appears instead of the orthorhombic CrB-type structure, the texturing of orthorhombic CrB and monoclinic TiNi may testify that crystallographic planes (010) CrB and (100) TiNi are parallel.

Hence, X-ray diffraction of the $Zr_{50}Co_{25}Ni_{25}$ alloy in the range 30–800°C has revealed the following sequence of phase transformations of martensitic nature: $\delta''(\text{CrB}) \rightarrow \delta'(\text{AuCu}) \rightarrow \delta(\text{CsCl})$ when the sample is heated and $\delta'(\text{CsCl}) \rightarrow \delta'''(\text{TiNi})$ when the sample is cooled down. Difference in the transformations during heating and cooling testifies that annealing influences the martensitic phase structure. The orthorhombic CrB-type phase was the final product of martensitic transformation in the as-cast alloy. The monoclinic TiNi-type phase resulted from martensitic transformation of the annealed sample.

CONCLUSIONS

High-temperature X-ray diffraction has been employed to examine variations in the crystal structure of the $Zr_{50}Co_{25}Ni_{25}$ alloy over a range from room temperature to 800°C. It is shown that the starting alloy has a single phase with orthorhombic CrB-type structure at room temperature.

When temperature increases to 400°C and 600°C, the low-symmetry orthorhombic phase gradually transforms to the tetragonal phase with AuCu-type structure. The high-symmetry cubic structure of CsCl type peculiar to ZrCo shows up at 800°C. At this temperature, this structure is in equilibrium with the monoclinic TiNi-type phase that remains when the sample is cooled down to 30°C.

REFERENCES

1. D. Hossain and J. R. Harris, "A study of ZrCo and related ternary phases represented by the general formula $Zr_{50}Co_{50-x}Ni_x$," *J. Less-Common Met.*, **37**, 35–37 (1974).
2. C. Lall, M. H. Lorello, and J. R. Harris, "Transformation and deformation studies of some Zr(CoNi) alloys," *Acta Metall.*, **26**, 1631–1641 (1978).
3. E. M. Carvalho, "Magnetic susceptibility studies of phase transformations in the system $Zr_{50}Co_{50-x}Ni_x$ ($0 \le \le x \le 50$): I," *J. Less-Common Met.*, **106**, 117–128 (1985).
4. E. M. Carvalho and J. R. Harris, "Electrical resistivity studies of phase transformations in the system $Zr_{50}Co_{50-x}Ni_x$ ($0 \le x \le 50$): II," *J. Less-Common Met.*, **106**, 129–141 (1985).
5. E. M. Carvalho and J. R. Harris, "X-ray diffraction studies of structural changes in the system $Zr_{50}Co_{50-x}Ni_x$ ($0 \le x \le 50$): III," *J. Less-Common Met.*, **106**, 143–152 (1985).
6. M. Matsuda, K. Hayashi, and M. Nishida, "Ductility enhancement in B2-type Zr–Co–Ni alloys with martensitic transformation," *Mater. Trans.*, **50**, No. 9, 2335–2340 (2009).
7. M. Matsuda, K. Hayashi, and K. Nishida, "Microstructure and mechanical properties of Zr–Co–Ni intermetallic compound," *Mater. Sci. Forum*, **638–642**, 1379–1383 (2010).
8. M. Matsuda, T. Nishimoto, K. Matsunaga, et al., "Deformation structure in ductile B2 type Zr–Co–Ni alloys with martensitic transformation," *J. Mater. Sci.*, **46**, 4221–4227 (2011).
9. M. Matsuda, Y. Iwamoto, Y. Morizono, et al., "Enhancement of ductility in B2-type Zr–Co–Ni alloys with deformation-induced martensite and microcrack formation," *Intermetallics*, **36**, 45–50 (2013).
10. Yu. N. Koval, G. S. Firstov, J. V. Humbeeck, et al., "B2 Intermetallic compounds of Zr. New class of the shape memory alloys," *J. Phys. IV*, **5**, C8-1103–C8-1108 (1995).
11. Yu. N. Koval, "High-temperature shape memory effect in some alloys and compounds," in: *Mater. Sci. For. Proc. Inter. Symp. Shape Memory Materials* (May, 1999, Kanazama, Japan), Kanazama, Japan (2000), Vol. 327–328, pp. 271–278.

12. T. A. Kosorukova, G. S. Firstov, Yu. N. Koval, V. G. Ivanchenko, et al., “Phase transformations in intermetallics $Zr_{50}Co_{50-x}Ni_x$ ($0 < x < 50$),” *Dop. Nats. Akad. Nauk Ukrainy*, No. 12, 114–121 (2012).
13. V. N. Eremenko, E. L. Semenova, and T. D. Shtepa, “Study of transformations in near-equiatomic Zr–Rh alloys,” in: *Thermal Analysis and Phase Equilibria* [in Russian], Perm (1983), pp. 109–113.
14. J. K. Stalick, L. A. Bendersky, and P. M. Waterstvat, “One-dimensional disorder in Zr_9Ni_{11} (M = Ni, Pd, Pt) and low temperature atomic mobility in Zr_9Ni_{11},” *J. Phys. Condens. Matter*, **20**, No. 28, 285–309 (2008).
15. E. L. Semenova, “On constitution of the ZrCo–ZrNi alloys,” in: *Proc. 3rd Int. Conf. HighMatTech* (October 3–7, 2011, Kyiv), Kyiv (2011), p. 279.
16. V. N. Khachin, “Martensitic inelasticity of alloys,” *Izv. Vus. Fiz.*, No. 5, 88–103 (1985).